Silencing Cenp-F weakens centromeric cohesion, prevents chromosome alignment and activates the spindle checkpoint

Sarah V. Holt, Mailys A. S. Vergnolle, Deema Hussein*, Marcin J. Wozniak, Victoria J. Allan and Stephen S. Taylor‡

Faculty of Life Sciences, University of Manchester, The Michael Smith Building, Oxford Road, Manchester, M13 9PT, UK
*Present address: Paterson Institute for Cancer Research, Christie Hospital, Wilmslow Road, Manchester, M20 4BX, UK
‡Author for correspondence (e-mail: stephen.taylor@manchester.ac.uk)

Accepted 3 August 2005
Journal of Cell Science 118, 4889-4900 Published by The Company of Biologists 2005
doi:10.1242/jcs.02614

Summary

Cenp-F is an unusual kinetochore protein in that it localizes to the nuclear matrix in interphase and the nuclear envelope at the G2/M transition; it is farnesylated and rapidly degraded after mitosis. We have recently shown that farnesylation of Cenp-F is required for G2/M progression, its localization to kinetochores, and its degradation. However, the role Cenp-F plays in mitosis has remained enigmatic. Here we show that, following repression of Cenp-F by RNA interference (RNAi), the processes of metaphase chromosome alignment, anaphase chromosome segregation and cytokinesis all fail. Although kinetochores attach to microtubules in Cenp-F-deficient cells, the oscillatory movements that normally occur following K-fibre formation are severely dampened. Consistently, inter-kinetochore distances are reduced. In addition, merotelic associations are observed, suggesting that whereas kinetochores can attach microtubules in the absence of Cenp-F, resolving inappropriate interactions is inhibited. Repression of Cenp-F does not appear to compromise the spindle checkpoint. Rather, the chromosome alignment defect induced by Cenp-F RNA interference is accompanied by a prolonged mitosis, indicating checkpoint activation. Indeed, the prolonged mitosis induced by Cenp-F RNAi is dependent on the spindle checkpoint kinase BubR1. Surprisingly, chromosomes in Cenp-F-deficient cells frequently show a premature loss of chromatid cohesion. Thus, in addition to regulating kinetochore-microtubule interactions, Cenp-F might be required to protect centromeric cohesion prior to anaphase commitment. Intriguingly, whereas most of the sister-less kinetochores cluster near the spindle poles, some align at the spindle equator, possibly through merotelic or lateral orientations.

Supplementary material available online at
http://jcs.biologists.org/cgi/content/full/118/20/4889/DC1

Key words: Mitosis, Kinetochore, Cenp-F, Mitosin, Bub1, Sgo1, Cohesion, Merotelic

Introduction

Centromere protein-F (Cenp-F), originally identified as a human autoantigen, is part of the nuclear matrix during interphase and localizes to kinetochores during mitosis (Casiano et al., 1993; Rattner et al., 1993; Liao et al., 1995; Zhu et al., 1995b). Cenp-F remains kinetochore associated until anaphase, when it re-localizes to the spindle midzone. Cenp-F is regulated by the cell cycle, reaching maximum levels in G2/M, followed by rapid degradation after mitosis (Liao et al., 1995; Zhu et al., 1995b). A Cenp-F variant, termed mitosin, was identified in a screen for Rb interactors (Zhu et al., 1995b). Mitosin and Cenp-F are virtually identical and it is now accepted that they are one and the same (Yang et al., 2005). For clarity, we will refer to both as Cenp-F.

Cenp-F is a 3210 amino acid protein, comprising mainly coiled coil sequence, two internal repeats and several leucine heptad repeats (Liao et al., 1995). The kinetochore localization domain and a bipartite nuclear localization sequence reside in the C-terminal region (Zhu et al., 1995a). In yeast two-hybrid assays, the C-terminal domain of Cenp-F interacts with itself, the kinesin-related motor protein Cenp-E, and the spindle checkpoint component Bub1 (Zhu et al., 1995a; Chan et al., 1998; Jablonski et al., 1998), which is consistent with roles in chromosome segregation and/or spindle checkpoint control.

Proteins with homology to Cenp-F have been identified in yeast, worms, chickens and mice. The extreme C-terminus of Cenp-F shares 38% sequence identity with cardiac muscle factor 1 (CMF-1), a chicken protein expressed transiently in differentiating myogenic cells (Wei et al., 1996). Murine Lek1 is related to CMF-1 (Goodwin et al., 1999), and binds the pocket proteins, including Rb (Ashe et al., 2004). The significance of these homology relationships is unclear, but they may explain why mitosin was identified in a screen for Rb interactors (Zhu et al., 1995b). Okp1, from *Saccharomyces cerevisiae,* shares homology with the C-terminal domain of Cenp-F. Although its function is unknown, Okp1 is part of the yeast kinetochore complex (Ortiz et al., 1999; De Wulf et al., 2003). HCP-1 and HCP-2, kinetochore proteins in

Caenorhabditis elegans, share homology with the central repeats of Cenp-F and are required for normal chromosome segregation (Moore et al., 1999). Significantly, HCP-1/2 target CLASP to kinetochores in the developing *C. elegans* embryo, thereby facilitating microtubule polymerization at kinetochores (Cheeseman et al., 2005). Whether Okp1 or HCP-1/2 are orthologues or paralogues of Cenp-F is unclear.

The Cenp-F protein sequence ends with a CAAX farnesylation motif and Cenp-F is indeed farnesylated (Ashar et al., 2000). Consistent with protein farnesylation as a membrane-targeting signal, Cenp-F localizes to the nuclear envelope in late G2 (Hussein and Taylor, 2002). Interestingly, farnesylation of Cenp-F is required for its localization to the nuclear envelope, its ability to target kinetochores, and its degradation after mitosis (Hussein and Taylor, 2002). Importantly, ectopic expression of the C-terminus of Cenp-F delays cell-cycle progression in G2 (Zhu et al., 1995b; Hussein and Taylor, 2002). This delay is dependent on the CAAX motif, suggesting that farnesylation of Cenp-F is required for G2 progression (Hussein and Taylor, 2002), possibly explaining why farnesyl transferase inhibitors delay G2/M progression in some human tumour lines (Vogt et al., 1997; Ashar et al., 2001; Crespo et al., 2001).

The localization of Cenp-F, plus its similarity with Okp1 and HCP-1/2, suggests that it might also be required for chromosome segregation in human cells. Indeed, several kinetochore proteins and mitotic regulators, including Cenp-I, Sgt1, Zwint1, Bub1 and RanBP2, are required for kinetochore localization of Cenp-F (Liu et al., 2003; Johnson et al., 2004; Joseph et al., 2004; Steensgaard et al., 2004; Yang et al., 2005). Interestingly, Cenp-F is a target of FoxM1, a transcription factor required for chromosome stability in mammalian cells (Laoukili et al., 2005). Indeed, a recent report showed that chromosome alignment is inhibited following repression of Cenp-F by RNA interference (RNAi) (Yang et al., 2005). In this particular study, levels of kinetochore-bound Cenp-E and dynactin were shown to be reduced in Cenp-F-deficient cells, suggesting that the alignment defect was a consequence of abnormal motor function. Here, we confirm and extend these observations: we show that silencing Cenp-F in HeLa cells using RNAi inhibits chromosome alignment and activates the spindle checkpoint. The alignment defect is not because kinetochores cannot attach microtubules, but rather because kinetochores do not correctly biorient. Intriguingly, the absence of Cenp-F causes some sisters to undergo a premature loss of centromeric cohesion, similar to the phenotype observed following repression of Sgo1 (Salic et al., 2004; Tang et al., 2004; Kitajima et al., 2005; McGuinness et al., 2005).

Materials and Methods

Molecular cell biology

The experimental procedures used here have been extensively described elsewhere. Specifically, cell lines, culture conditions and drugs were all as described (Johnson et al., 2004). Cenp-F and BubR1 short interfering (si)RNA duplexes, plus transfection conditions, were as described (Johnson et al., 2004). The siRNA duplexes to repress Sgo1 were as described (Salic et al., 2004). Cenp-F immunoblots were as described (Hussein and Taylor, 2002) except that proteins were transferred onto nitrocellulose membranes as described (Tighe et al., 2004). Immunofluorescence analysis was carried out as described (Johnson et al., 2004). In addition to the previously described antibodies, the following were used: mouse monoclonal anti-Hec1 (Abcam; 1:500); rabbit polyclonal anti-Cenp-A (Upstate; 1:100); human polyclonal anti-centromere antibodies (ACA; kind gift from W. Earnshaw, ICMB, Edinburgh, UK; 1:800). A stable cell line expressing green fluorescent protein (GFP)-tagged Sgo1 was generated using the Flp-In^{TM} system (Invitrogen) as described previously (Johnson et al., 2004; Tighe et al., 2004). Time-lapse microscopy using a HeLa cell line expressing a GFP-tagged histone H2B was performed as described (Morrow et al., 2005). MPM-2 staining was as described (Johnson et al., 2004) except that the analysis was performed using a CyAn^{TM} flow cytometer (DakoCytomation). Preparation of metaphase spreads was as described (Tighe et al., 2004), whereas preparation of aqueous spreads for antibody labelling was as described previously (Tighe et al., 2001).

Analysis of K-fibres

Following RNAi, HeLa cells were seeded on coverslips and cultured for 24 hours. Cells were washed twice in PBS, permeabilized for 90 seconds in microtubule-stabilizing buffer (100 mM PIPES pH 6.8, 1 mM MgCl, 0.1 mM $CaCl_2$, 0.1% Triton X-100) at room temperature, then fixed for 10 minutes in 4% formaldehyde diluted in the microtubule-stabilizing buffer. Following washes in PBST (PBS plus 0.1% Triton X-100), cells were blocked in PBST plus 5% non-fat dried milk (Marvel) and incubated with primary antibodies (TAT-1, mouse anti-tubulin, 1:100; SB1.3, sheep anti-Bub1, 1:1000; ACA, human anti-centromere, 1:800) for 30 minutes at room temperature. Following washes in PBST, cells were incubated with secondary antibodies (Cy2 donkey anti-mouse, Cy3 donkey anti-sheep, Cy5 donkey anti-human) for 30 minutes at room temperature. Following washes in PBST, the cells was counterstained with Hoechst 33258 at 1 μg/ml for 5 minutes in PBST, mounted in 90% glycerol plus 20 mM Tris HCl pH 8.0 and briefly stored at –20°C. Deconvolution microscopy was performed using a widefield optical sectioning microscope (DeltaVision, Applied Precision) with immersion oil of refractive index 1.518. For each cell, a z-series of 40-50 images at 0.2 μm intervals was captured then processed using seven rounds of constrained iterative deconvolution. Deconvolved image stacks were projected using SoftWorx (Applied Precision).

Microtubule pelleting assay

Nocodazole-arrested HeLa cells were washed in BRB80 (80 mM PIPES pH 6.8, 2 mM $MgCl_2$, 1 mM EGTA) then lysed on ice for 20 minutes in 50 mM HEPES pH 7.5, 10% glycerol, 1% Triton X-100, 1.5 mM $MgCl_2$, 1 mM EGTA. The lysate was centrifuged at 100,000 ***g*** for 1 hour at 4°C, and the supernatant then diluted with 1 volume of BRB80 and supplemented with 10 U/ml hexokinase, 20 μM glucose, 20 μM taxol, 400 μM AMP-PNP, 1 mM DTT, 1 μg/ml cytochalasin D and protease inhibitors. After incubating for 10 minutes at room temperature, 40 μg taxol-stabilized microtubules were added, followed by incubation at room temperature for 30 minutes. The mix was then layered over a 600 μl sucrose cushion (40% in BRB80 supplemented with 4 μM taxol, 1 mM DTT, 1 μg/ml cytochalasin D, and protease inhibitors) and centrifuged at 68,000 ***g*** for 25 minutes at 30°C. The microtubule pellet was then incubated in 20 μl ATP-release buffer (BRB80 containing 5 mM ATP, 1 mM DTT, 4 μM taxol, 1 μg/ml cytochalasin D), incubated for 25 minutes at room temperature, then re-centrifuged at 68,000 ***g*** for 15 minutes at 30°C. The supernatant, containing a proportion of microtubule motors released from the pellet by ATP, was collected. A further 20 μl of release buffer was added to the pellet and immediately centrifuged as above. The original lysate, the cushion, the ATP-release and the microtubule pellet fraction were all then resuspended in sample buffer and analysed by immunoblotting as above.

Results

Cenp-F is required for metaphase chromosome alignment

To investigate the function of Cenp-F, we transfected HeLa cells with siRNA duplexes that we have previously shown to repress Cenp-F (Johnson et al., 2004). Immunoblotting demonstrated that Cenp-F was efficiently repressed (Fig. 1A). Immunofluorescence analysis showed that, in approximately 65% of cells, Cenp-F was largely depleted from kinetochores (Fig. 1B,C). Measurement of pixel intensities in these cells revealed that kinetochore-bound Cenp-F was reduced to approximately 6% (Johnson et al., 2004). Examination of Cenp-F-depleted mitotic cells immediately indicated that Cenp-F RNAi affected mitosis and/or cell division. For example, in the Cenp-F-deficient cell shown in Fig. 1C, there appear to be three masses of chromosomes, suggesting that this cell may have a tripolar spindle. Indeed, when we analysed spindle morphology using Aurora A as a pole marker (Fig. 1D), multipolar spindles were three times more prevalent than in control cells (Fig. 1E). As these cells were analysed 48 hours post-transfection, the simplest explanation for the multipolar spindle phenotype is that repression of Cenp-F inhibits chromosome segregation and/or cytokinesis, thus yielding cells with multiple centrosomes.

To determine if Cenp-F is required for chromosome segregation, we analysed chromosome morphology following Cenp-F RNAi. Mitosis was frequently abnormal in Cenp-F-deficient cells (Fig. 2A). Tight metaphase and anaphase figures were rarely apparent, and instead the chromosomes were distributed over a much larger area. A frequent phenotype can be seen in Fig. 2A panels v and vi (see also Fig. 5A, Fig. 6 and Fig. 8A panel iii) where some chromosomes appeared to form a broad metaphase plate, whereas others were clustered around the spindle poles.

To define the defect more precisely, we set out to quantitate the number of cells in the various mitotic stages. However, because of the defect, it was difficult to stage mitotic cells using chromosome morphology alone. Therefore, we stained cells to detect Aurora B, a chromosome passenger protein that localizes to centromeres in prometaphase and the spindle midzone in anaphase (reviewed by Carmena and Earnshaw, 2003). Following repression of Cenp-F, Aurora B foci were readily detectable on the chromosomes, indicating that Cenp-F is not required to target Aurora B to the centromere (Fig. 2B). Quantitation of pixel intensities confirmed that the levels of centromeric Aurora B were normal in Cenp-F-deficient cells (Fig. 2C). In control cells, Aurora B was readily detectable at both spindle midzones in anaphase and midbodies in telophase (Fig. 2B). By contrast, Aurora B-positive spindle midzones and midbodies were rarely observed following repression of Cenp-F. Indeed, based on both chromosome morphology and Aurora B localization, we determined that the number of anaphases was reduced to ~36% in Cenp-F-deficient populations (Fig. 2D).

The apparent reduction of anaphases following Cenp-F RNAi raises two possibilities: either chromosome alignment is normal, but segregation then fails; or alternatively Cenp-F repression directly inhibits chromosome alignment. Because normal metaphase figures were less abundant following repression of Cenp-F, we favoured the latter possibility. However, we were concerned that if Cenp-F RNAi compromised the spindle checkpoint, perhaps the cells were exiting mitosis before being able to align their chromosomes. Therefore, we treated cells with the proteasome inhibitor MG132 to prevent anaphase onset and mitotic exit downstream of the spindle checkpoint. Within one hour, the proportion of metaphases in control cultures increased sharply to ~65% (Fig. 2E), consistent with MG132 preventing the metaphase-

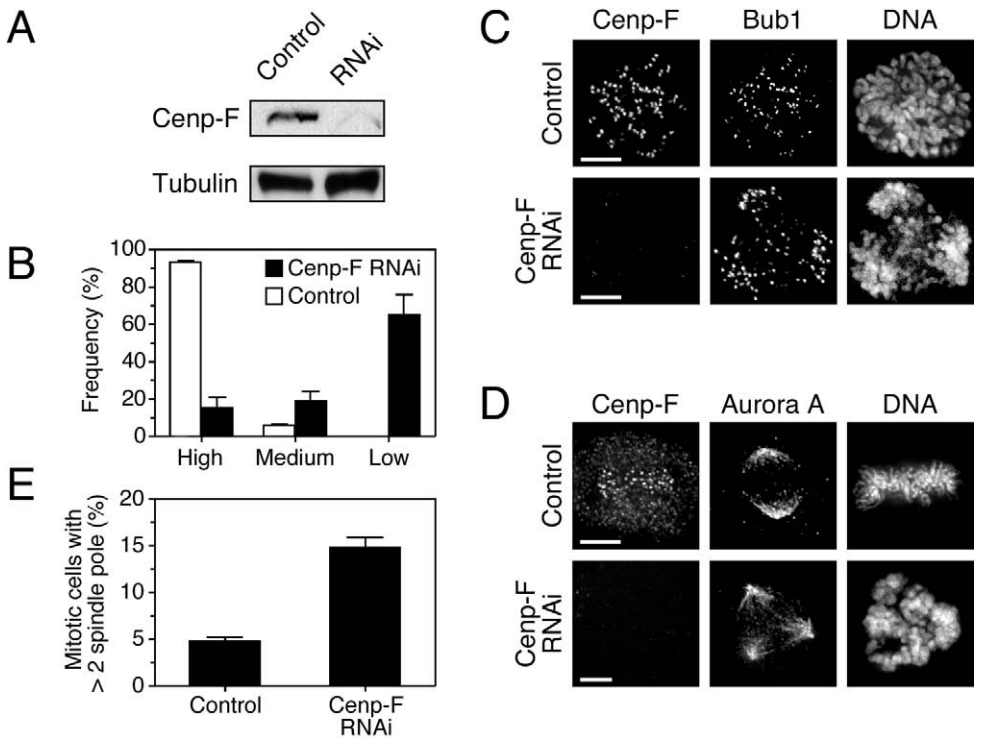

Fig. 1. Cenp-F is required for cell division. HeLa cells were transfected with siRNA duplexes then analysed 48 hours later by immunoblotting and immunofluorescence. (A) Immunoblot showing effective repression of Cenp-F, with tubulin acting as a loading control. (B) Quantitation of at least 100 mitotic cells by immunofluorescence scoring the levels of kinetochore-bound Cenp-F as either high, medium or low. (C) Images of mitotic cells showing that Cenp-F and Bub1 colocalize at kinetochores in control cells, but that Cenp-F is absent from kinetochores in Cenp-F RNAi cells; bar, 5 μm. (D) Images of mitotic cells stained to detect Cenp-F and Aurora A showing a tripolar spindle in the Cenp-F-deficient cell; bar, 5 μm. (E) Quantitation of mitotic cells with two or more spindle poles. In the bar graphs, values represent the mean±s.e.m. of three independent experiments in which at least 100 mitotic cells were counted.

anaphase transition and mitotic exit. However, in Cenp-F-repressed cultures, the proportion of metaphases rose only gradually, finally reaching ~55% after three hours (Fig. 2E). (Note that these metaphases were not as 'tight' as in control cells and inter-kinetochore distances were reduced; see below.) Thus, when mitotic progression is blocked downstream of the spindle checkpoint, repression of Cenp-F reduces the accumulation of metaphases, indicating that Cenp-F is indeed required for metaphase chromosome alignment.

Silencing Cenp-F activates the spindle checkpoint

To confirm the observations based on fixed cells, we used time-lapse microscopy to analyse mitosis. To visualize the chromatin in living cells directly, we generated a HeLa cell line expressing a GFP-tagged histone protein. Consistent with our analysis of DLD-1 cells expressing the same GFP-histone fusion (Morrow et al., 2005), control HeLa cells rapidly progressed from prometaphase to metaphase, then segregated their chromosomes within approximately 30 minutes (Fig. 3A and see supplementary material Movie 1). By contrast, many of the cells in Cenp-F RNAi cultures never formed distinct metaphase plates (Fig. 3A and see supplementary material Movies 2, 3 and 4). Although the chromosomes do move, the normal oscillatory movements observed in control cells were not apparent. Rather, the movements were either small, Brownian-type movements of individual chromosomes, or movement of the entire chromosome mass within the cell. Following a prolonged period, the cells eventually exited mitosis without any recognizable anaphase movement. The chromosomes then decondensed, forming multinucleated cells (Fig. 3A). Thus, the time-lapse data confirms the fixed cell data: Cenp-F is required for metaphase chromosome alignment.

Whereas control cells typically entered anaphase within 20-40 minutes, Cenp-F-deficient cells remained in mitosis for several hours (Fig. 3B). Consistently, repression of Cenp-F elevated the mitotic index of asynchronous populations (see below). This suggests that, in the absence of Cenp-F, the spindle checkpoint is activated. To test this directly, we co-repressed Cenp-F and an essential component of the spindle

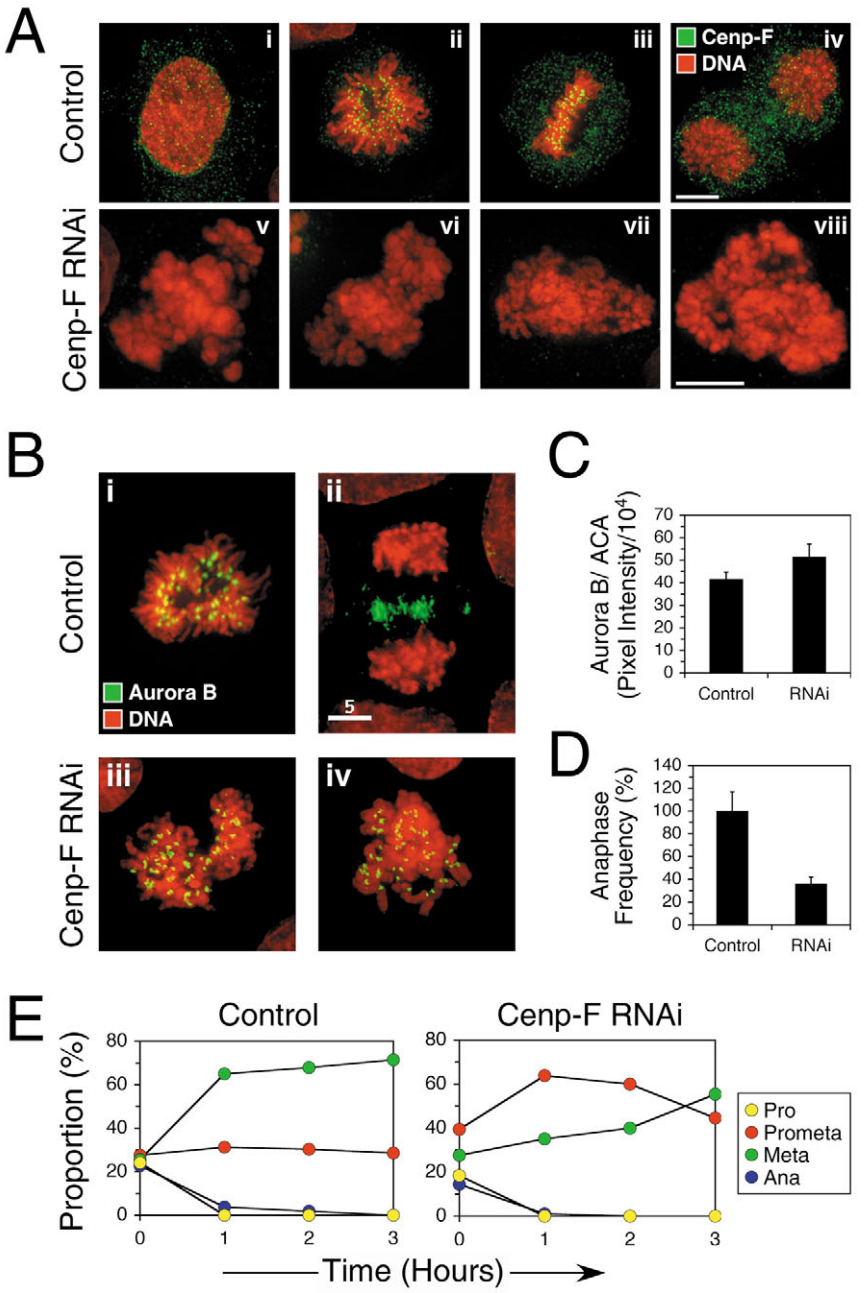

Fig. 2. Cenp-F is required for metaphase chromosome alignment. HeLa cells were transfected with siRNA duplexes then analysed 48 hours later by immunofluorescence. (A) Images of mitotic cells stained to detect Cenp-F (green) and the DNA (red), showing normal prophase, prometaphase, metaphase and anaphase configurations in control cells, and aberrant configurations in Cenp-F-deficient cells; bar, 5 μm. (B) Mitotic cells stained to detect Aurora B (green) and the DNA (red). Control cells show that Aurora B localizes to centromeres (panel i) and spindle midzones (panel ii). In Cenp-F-deficient cells, Aurora B localizes to centromeres but midzones and midbodies are rarely seen; bar, 5 μm. (C) Quantitation of pixel intensities showing that Cenp-F is not required for centromere localization of Aurora B. Values represent the mean±s.e.m. from ten well resolved kinetochores in three different cells. (D) Quantitation showing that repression of Cenp-F reduces the frequency of anaphases to ~36%; the values represent the mean±s.e.m. of three independent experiments in which at least 100 mitotic cells were scored per experiment. (E) Proportion of prophases (yellow), prometaphases (red), metaphases (green) and anaphases (blue) following exposure to the proteasome inhibitor MG132; the values represent the mean±s.e.m. of three independent experiments in which at least 100 mitotic cells were analysed per experiment.

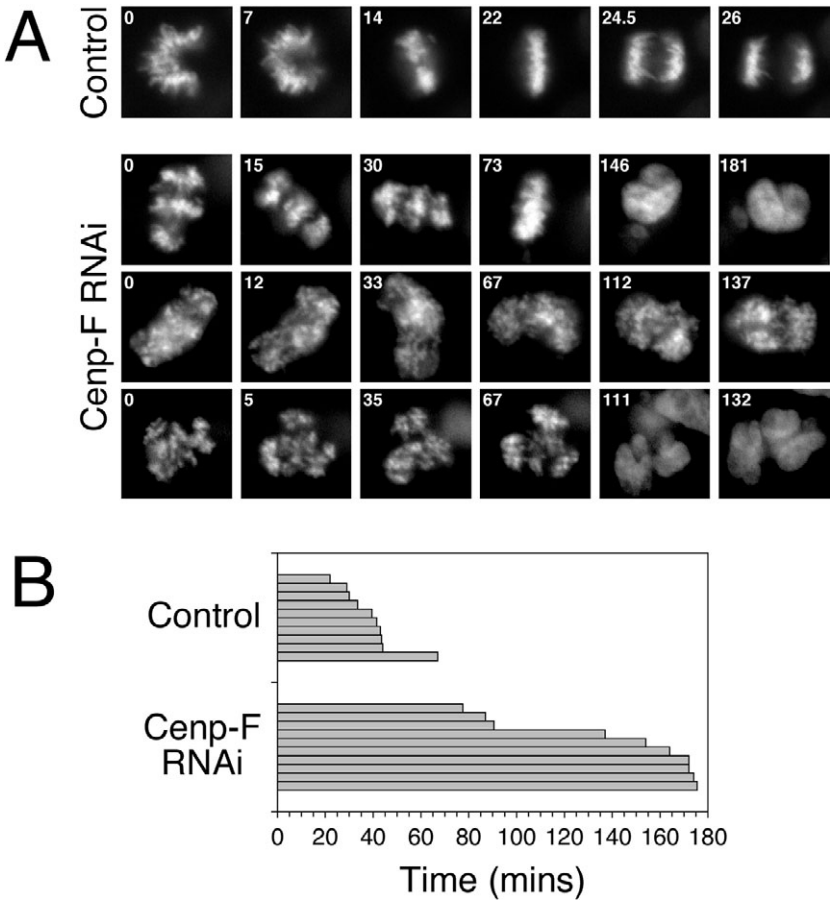

Fig. 3. Silencing Cenp-F delays mitotic exit. HeLa cells expressing a GFP-tagged histone H2B fusion protein were transfected with siRNA duplexes then analysed 48 hours later by time-lapse microscopy. (A) Images from time-lapse sequences showing normal chromosome alignment and segregation in a control cell, and aberrant mitoses in Cenp-F RNAi cultures. Numbers indicate time in minutes. (B) Graph showing the time in minutes from early prometaphase to mitotic exit showing that Cenp-F repression delays mitotic exit. Ten cells were analysed per group. Note that Cenp-F-deficient cells were identified by their aberrant chromosome morphologies, hence the time-lapse sequences start after prophase.

checkpoint, BubR1 (Fig. 4A). First, we quantitated the mitotic index in asynchronous populations, using MPM-2 as a mitotic marker. Consistent with delaying mitosis, the number of MPM-2-positive cells rose from ~2% in control cultures to ~5% in Cenp-F RNAi cultures (Fig. 4B). Consistent with spindle checkpoint override, the number of MPM-2-positive cells fell to ~1.5% in BubR1 RNAi cultures. Importantly, in the dual repressed culture, the number of MPM-2-positive cells was ~1.5%. Thus, BubR1 RNAi is dominant over Cenp-F RNAi, indicating that the delay induced by inhibiting Cenp-F is indeed due to spindle checkpoint activation.

To test this further, we analysed mitotic timing by time-lapse microscopy. The histogram plots in Fig. 4C clearly show that, whereas repression of BubR1 accelerated mitotic exit, repression of Cenp-F delayed mitotic exit. Importantly, the delay induced by Cenp-F RNAi was reduced when BubR1 was co-repressed. Specifically, whereas 27% of Cenp-F-repressed cells remained in mitosis for more than 80 minutes, when both BubR1 and Cenp-F were repressed, only 4% of the cells remained in mitosis for more than 80 minutes (Fig. 4C). This observation implies that Cenp-F is not itself required for spindle checkpoint function, despite the fact that it binds Bub1 in

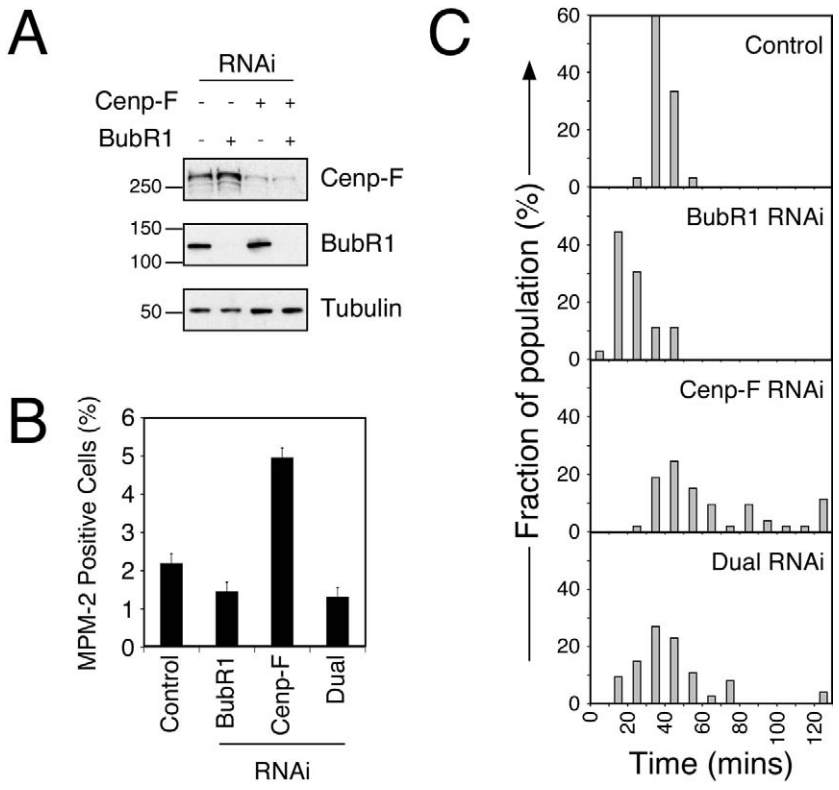

Fig. 4. Silencing Cenp-F activates the spindle checkpoint. HeLa cells were transfected with siRNA duplexes designed to repress both Cenp-F and BubR1 then analysed 48 hours later by immunoblotting, flow cytometry and time-lapse microscopy. (A) Blot showing efficient corepression of Cenp-F and BubR1. Numbers indicate size markers in kDa. (B) Bar graph quantitating the number of MPM-2-positive cells in asynchronous populations as determined by flow cytometric analysis of 10,000 cells. Values represent the mean±s.e.m. of three independent experiments. (C) Histograms plotting the time from nuclear envelope breakdown to anaphase. Number of cells analysed; Control, 33; BubR1 RNAi, 36; Cenp-F RNAi, 53; Dual RNAi, 74.

a yeast two-hybrid assay (Jablonski et al., 1998). Consistent with the notion that Cenp-F is not required for spindle checkpoint function, when Cenp-F RNAi cultures were exposed to nocodazole, cells accumulated in mitosis similar to controls (supplementary material Fig. S1). Furthermore, we have previously shown that Cenp-F is not required for kinetochore localization of Bub1, BubR1 or Mad2 (Johnson et al., 2004).

K-fibres form in the absence of Cenp-F

One possible explanation for the alignment failure in Cenp-F-deficient cells could be that Cenp-F is required to form stable kinetochore-microtubule interactions. To test this, we analysed K-fibre formation in control and Cenp-F-repressed cells. Prior to fixation, cells were extracted under conditions that result in the loss of astral and spindle microtubules, but preserve the more stable K-fibres (Mitchison et al., 1986). In control cells, metaphase spindles appeared very robust and K-fibres were clearly visible (Fig. 5A). Although the spindle structures appeared abnormal in Cenp-F-deficient cells (see below), microtubule fibres could be seen extending from the poles to the chromosomes, suggesting that K-fibres do form in the absence of Cenp-F. Consistent with this observation, Hec1/Nuf2, a component of the Ndc80 complex that is required for K-fibre formation (McCleland et al., 2004; DeLuca et al., 2005), localizes to kinetochores following depletion of Cenp-F (Fig. 5B).

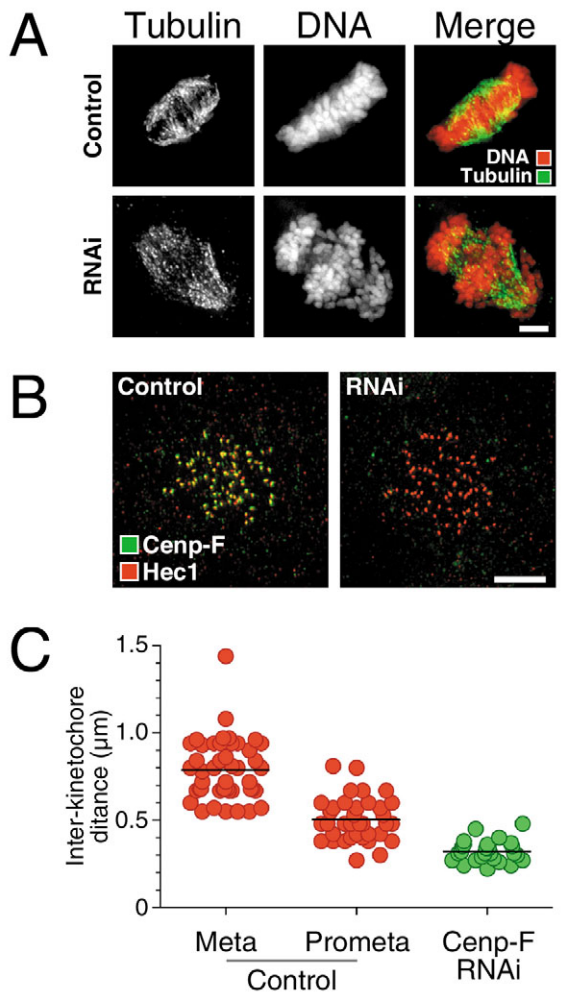

Fig. 5. K-fibres form in the absence of Cenp-F. (A) Control and Cenp-F RNAi cells were extracted to preserve K-fibres, then fixed and stained to detect tubulin (green) and the DNA (red). Note that although the spindle appears aberrant in Cenp-F-repressed cells, K-fibres are apparent. (B) Images of nocodazole-arrested cells stained to detect Cenp-F (green) and Hec1 (red) showing that Hec1 localizes to Cenp-F-depleted kinetochores. Scale bars represent 5 μm. (C) Graph plotting inter-kinetochore distances, in μm, using Cenp-A as a marker. Measurements are made using control cells in either prometaphase or metaphase, and Cenp-F deficient cells, horizontal lines represent the means.

Although kinetochores appear to attach microtubules in Cenp-F-deficient cells, the alignment defect, the broad metaphases and the time-lapse analysis (see above) suggest that kinetochore-microtubule interactions are not exerting the levels of tension required for coordinated chromosome movement. To test this, we measured inter-kinetochore distance using Cenp-A as a marker. In control prometaphase cells, the mean inter-kinetochore distance was ~0.5 μm (Fig. 5C). Consistent with tension increasing following biorientation, the inter-kinetochore distance of aligned control chromosomes was ~0.8 μm. Strikingly, in Cenp-F-deficient cells, the inter-kinetochore distance of chromosomes near the spindle equator was ~0.3 μm. Taken together, these observations suggest that, in the absence of Cenp-F, kinetochores can attach microtubules but the mechanisms that result in strong pulling forces across the kinetochores are seriously defective.

Note however that we could not determine the inter-kinetochore distance for all the chromosomes in Cenp-F-deficient cells, largely because many of the Cenp-A foci appeared as single spots rather than pairs (not shown but see below). Interestingly, whereas the single foci appeared clustered near the spindle poles, the paired foci tended to be near the spindle equator. As we describe below, Cenp-F RNAi weakens centromeric cohesion, suggesting that the chromosomes near the poles with single Cenp-A foci were probably individual chromatids that had prematurely lost sister chromatid cohesion.

Merotelic attachments form in the absence of Cenp-F

To characterize the alignment defects in more detail, we analysed Cenp-F-deficient cells using high-resolution 3D microscopy. Following RNAi, cells were extracted and fixed as above to preserve K-fibres, then stained to detect the chromosomes, microtubules, Bub1 and the centromeres. In control cells, bioriented kinetochore pairs were frequently observed with robust K-fibres terminating at kinetochores (Fig. 6A). Consistent with pulling forces exerting tension across the centromere, sister kinetochores near the edge of the spindle were up to 1 μm apart. Note that, in well-resolved examples, as shown in Fig. 6A, tubulin is not detectable between the kinetochores. Consistent with the inter-kinetochore distance measurements described above, highly stretched kinetochore pairs were not apparent in Cenp-F-deficient cells (Fig. 6B,C). Furthermore, it was difficult to find examples of truly bioriented chromosomes. For example, enlargement (a) in Fig.

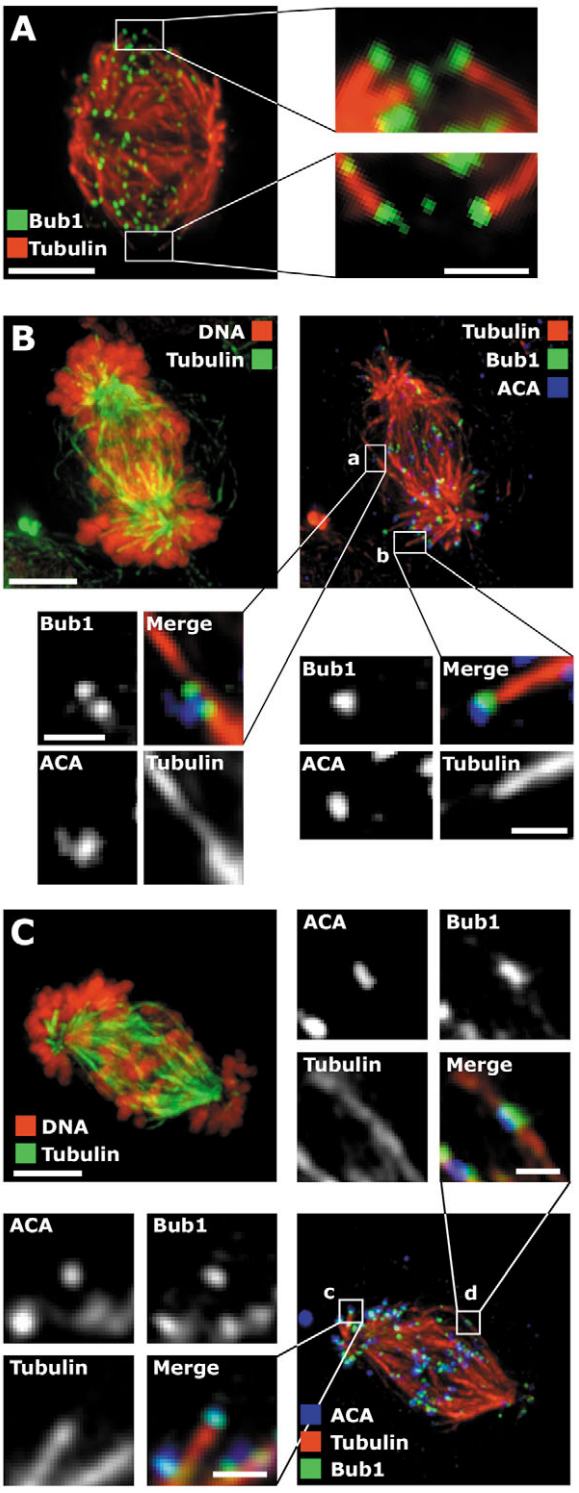

Fig. 6. Merotelic attachments form in the absence of Cenp-F. (A) Control metaphase stained to detect Bub1 (green) and tubulin (red), and enlargements showing examples of bioriented kinetochore pairs with K-fibres terminating at kinetochores. (B,C) Cenp-F-deficient cells stained to detect DNA (red), tubulin (green and red), Bub1 (green) and ACA (blue), as indicated. The enlargements show (a) a merotelic oriented kinetochore pair; (b,c) mono-oriented kinetochores lacking sisters; and (d) a merotelic oriented kinetochore that lacks a sister. Bar, 5 μm when the entire spindle is shown, and 1 μm in the enlargements.

6B shows an example of what appears to be a bioriented kinetochore pair where the inter-kinetochore distance is low. However, closer inspection indicates that there is no obvious break in the tubulin staining between the kinetochores. In addition, the centromere appears displaced to the side, rather than between the kinetochores. Therefore, this is probably a merotelic orientation, with one kinetochore attached to both poles, and the other attached to only one (supplementary material Fig. S2).

Consistent with the Cenp-A foci appearing as single spots rather than pairs (see above), single Bub1 foci often appeared clustered near the spindle poles (Fig. 6B,C, enlargements b and c), again suggesting that some chromatids had prematurely lost sister chromatid cohesion. Interestingly, whereas the single kinetochores were typically near the poles, we also observed single kinetochores near the spindle equator (Fig. 6C, enlargement d). These appeared to be attached to both poles, suggesting that the kinetochores on prematurely separated chromatids could align at the metaphase plate through either merotelic or lateral associations.

Cenp-F is required to maintain centromere cohesion

A consistent feature of both the fixed images and the time-lapse sequences of Cenp-F-deficient cells, were partial metaphases with a large number of chromosomes clustered near the spindle poles (Figs 2A, 3A, 5A and 8A). Because many of the chromosomes near the poles appeared to have only single kinetochore foci (Fig. 6B,C), we considered the possibility that perhaps some of the chromosomes in Cenp-F-deficient cells were undergoing a premature loss of sister chromatid cohesion. This might explain why some chromosomes, or rather chromatids, would cluster near the poles and would not be able to congress to the spindle equator. In addition, it would also explain why loss of Cenp-F function would result in spindle checkpoint activation (McGuinness et al., 2005).

To test this possibility, nocodazole-arrested cells were fixed in methanol/acetic acid and metaphase spreads were prepared. As a positive control, we repressed Sgo1 (Fig. 7A), a protein required to protect centromeric cohesion in both yeast and vertebrate cells (Katis et al., 2004; Kitajima et al., 2004; Marston et al., 2004; Rabitsch et al., 2004; Salic et al., 2004; Kitajima et al., 2005; McGuinness et al., 2005). As a negative control, we used siRNA duplexes that repress lamin B1 (Elbashir et al., 2001). In lamin B1 RNAi cultures, chromosome arms were well resolved, but the centromeres were typically closely associated, indicating that centromeric cohesion was intact (Fig. 7B). Consistent with previous observations (Salic et al., 2004; McGuinness et al., 2005), chromosomes in Sgo1 RNAi cultures frequently appeared as individual chromatids.

To confirm that these were in fact individual chromatids, we prepared aqueous spreads that are compatible with antibody labelling techniques. Whereas cohesed chromatids clearly had two kinetochores, as judged by Bub1 and ACA staining, what appeared to be individual chromatids, as judged by the DNA stain, only had single kinetochores, confirming that they were indeed separated chromatids (Fig. 7C). Premature loss of cohesion was also observed in Cenp-F RNAi cultures, although the phenotype appeared less penetrant, both qualitatively and quantitatively. For example, in some cells, whereas many

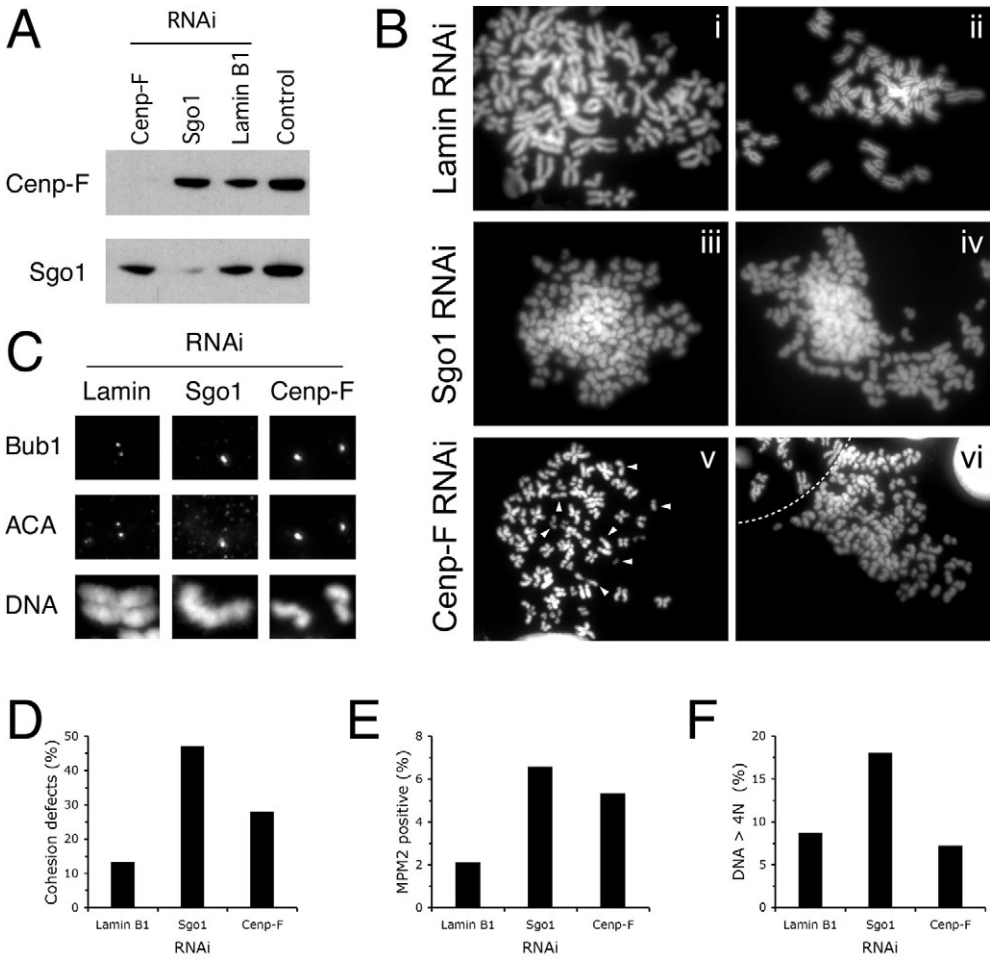

Fig. 7. Silencing Cenp-F weakens centromeric cohesion. HeLa cells were transfected with siRNA duplexes designed to repress lamin B1, Cenp-F and Sgo1. (A) Immunoblot showing repression of Cenp-F and Sgo1. (B) Metaphase spreads showing loss of centromere cohesion following repression of Cenp-F and Sgo1. Dashed line in panel (vi) separates chromosomes from two spreads. (C) Images of chromosomes stained with anti-Bub1 and anti-ACA antibodies confirming the presence of separated chromatids. (D) Bar graph quantitating the number of metaphase spreads with separated chromatids. At least 117 cells scored in each group. (E) Bar graph quantitating the number of MPM-2-positive cells in asynchronous populations, showing that repression of Cenp-F and Sgo1 activate the spindle checkpoint. (F) Bar graph quantitating the number of cells with DNA contents greater than 4N, showing that repression of Sgo1, but not Cenp-F, enhances endoreduplication.

chromosomes remained cohesed, individual chromatids were present (see arrow heads in Fig. 7B, panel v). Occasionally, the vast majority of chromosomes appeared to be separated chromatids (Fig. 7B, panel vi), similar to that observed following inhibition of Sgo1. Quantitation indicated that ~13% of lamin B1 and ~47% of the Sgo1 spreads contained single chromatids (Fig. 7D). Significantly, the number of cells with separated chromatids in Cenp-F RNAi spreads was twofold higher than that observed in the lamin B1 control (~28% versus 13%, Fig. 7D), which is consistent with the notion that Cenp-F RNAi does indeed weaken centromeric cohesion.

Cell fate following Cenp-F inhibition

As described previously (Salic et al., 2004; McGuinness et al., 2005), when Sgo1 was repressed, the mitotic index increased owing to spindle checkpoint activation (Fig. 7E). Similarly, repression of Cenp-F activated the spindle checkpoint (Fig. 4). Interestingly however, whereas the mitotic index increased in both the Sgo1 and Cenp-F RNAi cultures, endoreduplication – a downstream consequence of failure of cell division in p53-deficient cells – was more extensive in the Sgo1 culture (Fig. 7F). Interpreting these kinds of observations is complex (Rieder and Maiato, 2004), but it suggests that whereas Sgo1-deficient cells are competent to enter additional cell cycles following division failure, Cenp-F-deficient cells are less so. Whether this is a result of cell-cycle arrest in pseudo-G1, or the induction of apoptosis, remains to be seen.

The lack of endoreduplication seems at odds with our observation showing an increase in cells with multipolar spindles following Cenp-F RNAi (Fig. 1E). Notably, however, the increase in multipolar mitoses only reaches ~15% after 48 hours. Because mitosis seems to fail so frequently following Cenp-F RNAi (Fig. 2D), and because ~70% of the transfected cells are Cenp-F deficient (Fig. 1C), we would predict that more cells should have multiple spindle poles in the next mitosis. One possible explanation therefore is that the multipolar cells in the next mitosis are the rare survivors that continue cell-cycle progression despite mitotic exit in the absence of Cenp-F. Consistently, we observed few multinucleated cells following Cenp-F RNAi (supplementary material Fig. S3). Briefly, lamin B1, Cenp-F and Bub1 were repressed by RNAi then analysed 48 hours later. Consistent with Bub1 RNAi inducing an aberrant mitosis (Meraldi and Sorger, 2005; Morrow et al., 2005), ~63% of the cells were multinucleated. By contrast, in the Cenp-F RNAi culture, ~17% of cells were multinucleated, a value only marginally above the lamin B1 culture (~11%). This was surprising as the time-lapse analysis indicates that multinucleated cells are observed when Cenp-F-deficient cells exit mitosis (Fig. 3A). Presumably, therefore, these cells either reform a single nucleus or are lost from the population. Indeed, in light of the

report by Yang et al. (Yang et al., 2005), the simplest explanation to account for the low levels of endoreduplication and multinucleation observed following Cenp-F RNAi is that, following an aberrant mitosis, most Cenp-F-deficient cells do not continue cell-cycle progression.

Spindle assembly is aberrant in the absence of Cenp-F

In addition to the chromosome alignment defects observed in the absence of Cenp-F, spindle structure also appeared abnormal. Therefore, we analysed the structure of bipolar spindles in Cenp-F-depleted cells using conditions that preserve astral and spindle microtubules. In control cells, robust spindles were observed, with a high density of microtubules forming crescent shapes near the poles but decreasing towards the spindle midzone (Fig. 8A and see supplementary material Fig. S4). K-fibres, interdigitating spindle microtubules and astral microtubules were readily apparent. Although astral microtubules were apparent in Cenp-F-deficient cells, the rest of the spindle appeared abnormal (Fig. 8A). In particular, the crescent-shaped regions of high microtubule density were less apparent and were often cone shaped. The density of microtubules at the midzone appeared higher than in controls, with spindle microtubules often extending beyond the midzone. Quantitation of tubulin fluorescence signal along the spindle axis (see supplementary material Fig. S4) confirmed these observations. The graphs derived from control cells typically had two well-resolved peaks, with the peaks and the trough corresponding to the poles and midzone, respectively (Fig. 8B). By contrast, in Cenp-F deficient cells, the peaks and troughs were flatter because microtubule density was relatively lower at the poles and higher in the midzone (Fig. 8B).

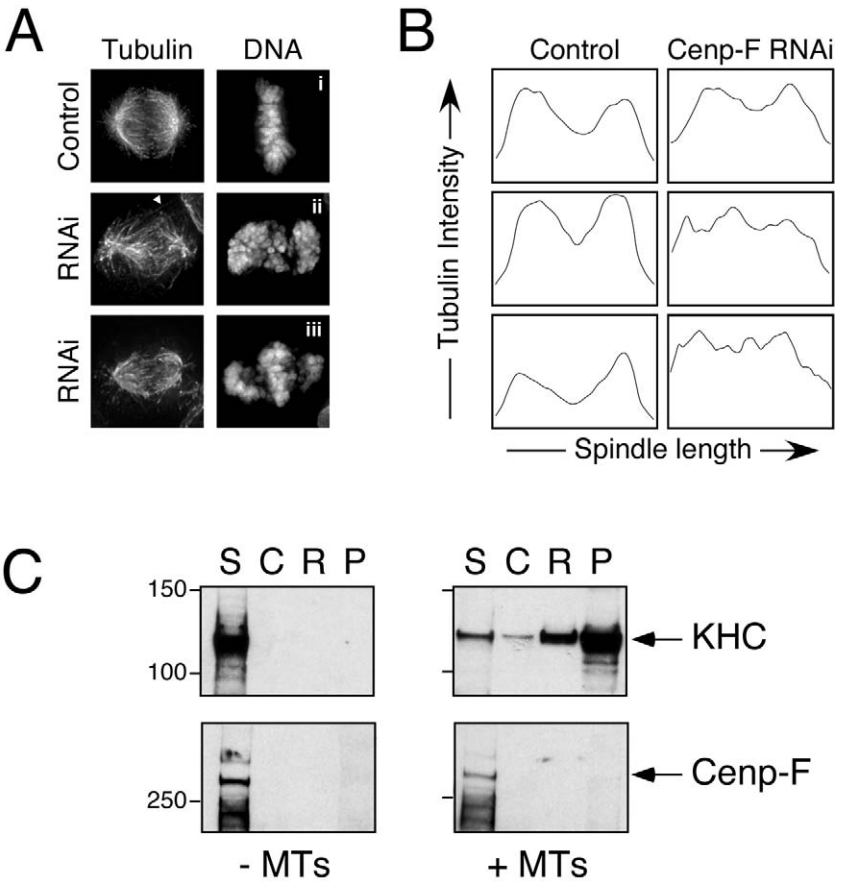

Fig. 8. Silencing Cenp-F results in aberrant spindle morphology. (A) Transfected HeLa cells were fixed under conditions that preserve all microtubules and were then stained to detect tubulin and the DNA. Images show representative spindles in control and Cenp-F-deficient cells. Arrowhead identifies an abnormally long microtubule extending beyond the spindle midzone. (B) Histograms plotting tubulin intensity along the spindle axis. (C) Microtubule pelleting assay showing that whereas kinesin heavy chain (KHC) binds taxol-stabilized microtubules, Cenp-F does not. S, supernatant (i.e. the cell lysate used for the assay); C, the sucrose cushion; R, the ATP-release fraction; P, the microtubule pellet. The assay was performed with (+MTs) and without (–MTs) microtubules, confirming that the pelleting of KHC is microtubule dependent.

Although it is possible that the 'weaker' spindle structures is a secondary consequence of the chromosome alignment defect, it is also possible that the spindle defects arise because Cenp-F is required for microtubule dynamics, independent of its role at kinetochores. Importantly, whereas Cenp-F localizes to kinetochores, a large pool is present in the cytosol. Furthermore, in anaphase, Cenp-F can be detected at the spindle midzone (Casiano et al., 1993; Rattner et al., 1993), suggesting that it might interact directly with microtubules. To test this, we incubated taxol-stabilized microtubules in protein lysates from nocodazole-arrested mitotic HeLa cells. The taxol-stabilized microtubules were then pelleted through a sucrose cushion, incubated in ATP to release a proportion of the microtubule motors and analysed by immunoblotting. Whereas kinesin heavy chain, a known microtubule-associated protein, was clearly detectable in both the microtubule-bound pellet fraction and the ATP-release fraction, Cenp-F was not (Fig. 8C). Although we cannot rule out the possibility that a small subpool of Cenp-F interacts directly with microtubules, possibly at kinetochores, Cenp-F does not appear to associate with microtubules in the cytosol. The mechanism underlying the abnormal spindle structure therefore remains unclear.

Discussion

Although Cenp-F was shown to be a kinetochore component over 10 years ago, its function has remained enigmatic. Here, we show that Cenp-F is required for mitotic chromosome segregation in human cells. Specifically, bipolar spindles and K-fibres form in Cenp-F-deficient cells (Fig. 5A), and although some chromosomes align at the spindle equator, inter-kinetochore distances are dramatically reduced (Fig. 5C), and normal chromosome movement is severely dampened (Fig. 3A). Consequently, the chromosomes at the spindle equator do not form tight metaphase plates typical of control cells (Fig. 2A, Fig. 3A, Fig. 5A, Fig. 8A). This phenotype can be

explained at least in part because some chromosomes at the spindle equator appear to be merotelically orientated in the absence of Cenp-F (Fig. 6). At the same time, some chromosomes appear to lose centromeric cohesion prematurely, yielding separated sister chromatids (Figs 6, 7), thereby accounting for the clustering of chromosomes around the spindle poles (Fig. 2A, Fig. 3A, Fig. 5A, Fig. 8A). Interestingly, however, some kinetochores lacking sisters do align at the spindle equator through merotelic associations. Probably as a direct consequence of the cohesion defect, the BubR1-dependent spindle checkpoint is activated (Fig. 4), delaying mitotic exit for up to several hours (Fig. 3B). Following a prolonged mitosis, Cenp-F-deficient cells return to interphase, without any signs of chromosome segregation. The long-term fate of these cells is not clear. The fact that multipolar spindles are observed suggest that some cells progress into another cell cycle (Fig. 1E). However, few Cenp-F-deficient cells endoreduplicate (Fig. 7F), suggesting that mitotic exit in the absence of Cenp-F might induce cell-cycle arrest or apoptosis.

Silencing Cenp-F inhibits chromosome movement

In *C. elegans* embryos, inhibition of the Cenp-F-related proteins HCP-1/2 prevents metaphase chromosome alignment (Moore et al., 1999; Cheeseman et al., 2005). A similar phenotype occurs following depletion of CLS-2, the *C. elegans* CLASP homologue, and importantly, HCP-1 and -2 target CLS-2 to the kinetochore (Cheeseman et al., 2005). If the function of HCP-1/2 is shared by Cenp-F, it is conceivable that the clustering of chromosomes near the poles in Cenp-F-deficient cells is because the kinetochores on mono-oriented chromosomes cannot undergo efficient away-from-pole (AP) movement. Indeed, when Cenp-F-deficient cells are cultured in MG132, the number of metaphases increases very slowly (Fig. 2E), suggesting that some chromosomes can biorient, but that congression is inhibited, consistent with an AP defect. For technical reasons, we have not yet been able to investigate whether Cenp-F is required for kinetochore localization of CLASP proteins in human cells. However, a CLASP defect does not seem sufficient to explain the Cenp-F RNAi phenotype fully. Indeed, it is not clear whether Cenp-F and HCP-1/2 are true orthologues. Note that, in contrast to Cenp-F, HCP-1/2 is required for spindle checkpoint function in *C. elegans* (Stear and Roth, 2004; Encalada et al., 2005). In addition, cohesion defects have not been reported following suppression of HCP-1/2.

Although we cannot rule out a CLASP defect, our observations suggest two other potential mechanisms to account for the alignment failure. First, we observed chromosomes where one kinetochore appeared to be attached to microtubules emanating from opposite spindle poles (Fig. 6). The presence of such merotelic orientations suggests that Cenp-F-deficient cells are unable to resolve inappropriate kinetochore-microtubule interactions. Although it appears that cells do have mechanisms to correct merotelic orientations (Cimini et al., 2003), the molecular events involved are far from clear. Recent evidence suggests that MCAK, a Kin I kinesin, may be involved (Kline-Smith et al., 2004), and our new data presented here implies a role for Cenp-F. A second mechanism contributing to the alignment defect comes from our observation showing that some chromatids prematurely loose cohesion in the absence of Cenp-F. In the absence of a sister, the ability to congress to the metaphase plate is clearly inhibited. Note however that congression of single kinetochores to the spindle equator is not impossible (Brinkley et al., 1988; Khodjakov et al., 1997). Indeed, we observed a sister-less kinetochore near the spindle equator attached to K-fibres emanating from opposite spindle poles. That paired and unpaired kinetochores can attach to both poles in the absence of Cenp-F might account for why we observed a slow increase in metaphase numbers when Cenp-F-deficient cells were exposed to MG132 (Fig. 2E).

Silencing Cenp-F weakens centromeric cohesion

A simple explanation to account for the clustering of chromosomes near the spindle poles is a cohesion defect. It is now clear, that in vertebrate cells, sister chromatid cohesion is lost in two phases (Nasmyth, 2002). Whereas arm cohesion is dissolved in prophase, cohesion at the centromere is protected until anaphase onset. Recently, members of the Sgo1/Mei-S332 family have emerged as key protectors of centromeric cohesion (Kerrebrock et al., 1992; LeBlanc et al., 1999; Katis et al., 2004; Kitajima et al., 2004; Marston et al., 2004; Rabitsch et al., 2004; Salic et al., 2004; McGuinness et al., 2005). We were struck by the similarity between the Cenp-F RNAi phenotype described here and that observed following repression of Sgo1 (Salic et al., 2004, Fig. 2C within) and (McGuinness et al., 2005, Fig. 6A,D within). We speculated therefore that Cenp-F RNAi might induce a cohesion defect. Consistent with this notion, metaphase spreads prepared from Cenp-F-deficient cultures show a significant fraction of prematurely separated chromatids (Fig. 7). This does not appear to be an artefact due to the preparation of chromosome spreads: kinetochores without sisters are clearly detectable clustered around the spindle poles in Cenp-F-deficient cells (Fig. 6). How Cenp-F might contribute to cohesion protection is unclear; preliminary analysis suggests that Sgo1 localizes to centromeres in the absence of Cenp-F (M.A.S.V., unpublished observation). However, repression of Sgo1 decreases kinetochore-bound Cenp-F and Cenp-E, but has no effect on Hec1 (Salic et al., 2004). Similarly, repression of Cenp-F reduces kinetochore-bound Cenp-E, but not Hec1. In addition, Bub1 is required for kinetochore localization of both Cenp-F and Sgo1 (Johnson et al., 2004; Tang et al., 2004; Kitajima et al., 2005). Thus, it is conceivable that Bub1, Sgo1 and Cenp-F are components of a common pathway that protects centromeric cohesion.

Silencing Cenp-F affects spindle morphology

Repression of Cenp-F by RNAi also appears to affect spindle assembly (Fig. 8), a phenomenon also reported by Yang et al. (Yang et al., 2005). Because Cenp-F did not pellet with taxol-stabilized microtubules (Fig. 8C), we feel that is unlikely that Cenp-F directly affects microtubule dynamics. Rather, we suspect that the apparent spindle defect is probably a consequence of the chromosome alignment/segregation defect. One possibility is that the presence of separated sister chromatids near the spindle poles imparts anaphase B type properties on the microtubules. Following sister chromatid

segregation during anaphase A, changes in microtubule flux and microtubule sliding at the spindle midzone causes spindle elongation during anaphase B (Brust-Mascher et al., 2004). Recent evidence from budding yeast suggests that changes in microtubule dynamics are coupled with the initiation of anaphase (Higuchi and Uhlmann, 2005). Specifically, separase activation, which triggers sister chromatid separation, activates the Cdc14 phosphatase, which in turn down regulates microtubule dynamics. Whether a similar mechanism occurs in human cells is not clear. However, it is conceivable that, by mimicking a normal anaphase, the clustering of separated chromatids near the spindle poles might affect microtubule dynamics, flux and/or sliding at the midzone. This in turn might account for the long microtubules and buckled spindles observed following repression of Cenp-F (Fig. 8A).

Concluding remarks

Inhibition of Cenp-F by RNAi clearly inhibits chromosome alignment and segregation. Indeed, the similarity between our study and the one recently described by Yang et al. (Yang et al., 2005) underscores the importance of Cenp-F in the chromosome alignment process. Because Cenp-F localizes to kinetochores and is homologous to Okp1 and HCP-1/2, it is tempting to speculate that these defects reflect a role for Cenp-F at the kinetochore. However, ectopic expression of the kinetochore-targeting domain of Cenp-F had little detectable effect on chromosome segregation, even though it displaced endogenous Cenp-F from kinetochores (Hussein and Taylor, 2002). Although the C-terminal domain of Cenp-F may be sufficient for its kinetochore function, it raises the possibility that Cenp-F has functions independent of the kinetochore. Indeed, only a small subpool of Cenp-F localizes to kinetochores. Taken together with the fact that Cenp-F is a very large, farnesylated protein that tightly binds the nuclear matrix in interphase and the nuclear envelope in G2, this suggests that there is still much to learn about the role Cenp-F plays in mediating chromosome segregation.

The authors thank Bill Earnshaw (Edinburgh) for ACA antibodies and Iain Cheeseman (San Diego) for communicating results prior to publication. We thank Anthony Tighe for the GFP-histone HeLa line, and Peter March and Jane Kott for advice on DeltaVision microscopy. S.V.H. thanks past and present members of the Taylor lab. S.S.T. thanks Andrew Holland and Pat Eyers for comments on the manuscript and encouragement. S.V.H. is supported by a studentship from the Medical Research Council, M.A.S.V. and M.J.W. are supported by the Biotechnology and Biological Sciences Research Council, and S.S.T. is a Cancer Research UK Senior Fellow.

References

Ashar, H. R., James, L., Gray, K., Carr, D., Black, S., Armstrong, L., Bishop, W. R. and Kirschmeier, P. (2000). Farnesyl transferase inhibitors block the farnesylation of CENP-E and CENP-F and alter the association of CENP-E with the microtubules. *J. Biol. Chem.* **275**, 30451-30457.

Ashar, H. R., James, L., Gray, K., Carr, D., McGuirk, M., Maxwell, E., Black, S., Armstrong, L., Doll, R. J., Taveras, A. G. et al. (2001). The farnesyl transferase inhibitor SCH 66336 induces a G(2) → M or G(1) pause in sensitive human tumor cell lines. *Exp. Cell Res.* **262**, 17-27.

Ashe, M., Pabon-Pena, L., Dees, E., Price, K. L. and Bader, D. (2004). LEK1 is a potential inhibitor of pocket protein-mediated cellular processes. *J. Biol. Chem.* **279**, 664-676.

Brinkley, B. R., Zinkowski, R. P., Mollon, W. L., Davis, F. M., Pisegna, M. A., Pershouse, M. and Rao, P. N. (1988). Movement and segregation of kinetochores experimentally detached from mammalian chromosomes. *Nature* **336**, 251-254.

Brust-Mascher, I., Civelekoglu-Scholey, G., Kwon, M., Mogilner, A. and Scholey, J. M. (2004). Model for anaphase B: role of three mitotic motors in a switch from poleward flux to spindle elongation. *Proc. Natl. Acad. Sci. USA* **101**, 15938-15943.

Carmena, M. and Earnshaw, W. C. (2003). The cellular geography of aurora kinases. *Nat. Rev. Mol. Cell Biol.* **4**, 842-854.

Casiano, C. A., Landberg, G., Ochs, R. L. and Tan, E. M. (1993). Autoantibodies to a novel cell cycle-regulated protein that accumulates in the nuclear matrix during S phase and is localized in the kinetochores and spindle midzone during mitosis. *J. Cell Sci.* **106**, 1045-1056.

Chan, G. K., Schaar, B. T. and Yen, T. J. (1998). Characterization of the kinetochore binding domain of CENP-E reveals interactions with the kinetochore proteins CENP-F and hBUBR1. *J. Cell Biol.* **143**, 49-63.

Cheeseman, I. M., Macleod, I., Yates, J. R., 3rd, Oegema, K. and Desai, A. (2005). The CENP-F-like proteins HCP-1 and HCP-2 target CLASP to kinetochores to mediate chromosome segregation. *Curr. Biol.* **15**, 771-777.

Cimini, D., Moree, B., Canman, J. C. and Salmon, E. D. (2003). Merotelic kinetochore orientation occurs frequently during early mitosis in mammalian tissue cells and error correction is achieved by two different mechanisms. *J. Cell Sci.* **116**, 4213-4225.

Crespo, N. C., Ohkanda, J., Yen, T. J., Hamilton, A. D. and Sebti, S. M. (2001). The farnesyltransferase inhibitor, FTI-2153, blocks bipolar spindle formation and chromosome alignment and causes prometaphase accumulation during mitosis of human lung cancer cells. *J. Biol. Chem.* **276**, 16161-16167.

DeLuca, J. G., Dong, Y., Hergert, P., Strauss, J., Hickey, J. M., Salmon, E. D. and McEwen, B. F. (2005). Hec1 and nuf2 are core components of the kinetochore outer plate essential for organizing microtubule attachment sites. *Mol. Biol. Cell* **16**, 519-531.

De Wulf, P., McAinsh, A. D. and Sorger, P. K. (2003). Hierarchical assembly of the budding yeast kinetochore from multiple subcomplexes. *Genes Dev.* **17**, 2902-2921.

Elbashir, S. M., Harborth, J., Lendeckel, W., Yalcin, A., Weber, K. and Tuschl, T. (2001). Duplexes of 21-nucleotide RNAs mediate RNA interference in cultured mammalian cells. *Nature* **411**, 494-498.

Encalada, S. E., Willis, J., Lyczak, R. and Bowerman, B. (2005). A spindle checkpoint functions during mitosis in the early Caenorhabditis elegans embryo. *Mol. Biol. Cell* **16**, 1056-1070.

Goodwin, R. L., Pabon-Pena, L. M., Foster, G. C. and Bader, D. (1999). The cloning and analysis of LEK1 identifies variations in the LEK/centromere protein F/mitosin gene family. *J. Biol. Chem.* **274**, 18597-18604.

Higuchi, T. and Uhlmann, F. (2005). Stabilization of microtubule dynamics at anaphase onset promotes chromosome segregation. *Nature* **433**, 171-176.

Hussein, D. and Taylor, S. S. (2002). Farnesylation of Cenp-F is required for G2/M progression and degradation after mitosis. *J. Cell Sci.* **115**, 3403-3414.

Jablonski, S. A., Chan, G. K., Cooke, C. A., Earnshaw, W. C. and Yen, T. J. (1998). The hBUB1 and hBUBR1 kinases sequentially assemble onto kinetochores during prophase with hBUBR1 concentrating at the kinetochore plates in mitosis. *Chromosoma* **107**, 386-396.

Johnson, V. L., Scott, M. I., Holt, S. V., Hussein, D. and Taylor, S. S. (2004). Bub1 is required for kinetochore localization of BubR1, Cenp-E, Cenp-F and Mad2, and chromosome congression. *J. Cell Sci.* **117**, 1577-1589.

Joseph, J., Liu, S. T., Jablonski, S. A., Yen, T. J. and Dasso, M. (2004). The RanGAP1-RanBP2 complex is essential for microtubule-kinetochore interactions in vivo. *Curr. Biol.* **14**, 611-617.

Katis, V. L., Galova, M., Rabitsch, K. P., Gregan, J. and Nasmyth, K. (2004). Maintenance of cohesin at centromeres after meiosis I in budding yeast requires a kinetochore-associated protein related to MEI-S332. *Curr. Biol.* **14**, 560-572.

Kerrebrock, A. W., Miyazaki, W. Y., Birnby, D. and Orr-Weaver, T. L. (1992). The Drosophila mei-S332 gene promotes sister-chromatid cohesion in meiosis following kinetochore differentiation. *Genetics* **130**, 827-841.

Khodjakov, A., Cole, R. W., McEwen, B. F., Buttle, K. F. and Rieder, C. L. (1997). Chromosome fragments possessing only one kinetochore can congress to the spindle equator. *J. Cell Biol.* **136**, 229-240.

Kitajima, T. S., Kawashima, S. A. and Watanabe, Y. (2004). The conserved kinetochore protein shugoshin protects centromeric cohesion during meiosis. *Nature* **427**, 510-517.

Kitajima, T. S., Hauf, S., Ohsugi, M., Yamamoto, T. and Watanabe, Y. (2005). Human Bub1 defines the persistent cohesion site along the mitotic chromosome by affecting Shugoshin localization. *Curr. Biol.* **15**, 353-359.

Kline-Smith, S. L., Khodjakov, A., Hergert, P. and Walczak, C. E. (2004). Depletion of centromeric MCAK leads to chromosome congression and segregation defects due to improper kinetochore attachments. *Mol. Biol. Cell* **15**, 1146-1159.

Laoukili, J., Kooistra, M. R., Bras, A., Kauw, J., Kerkhoven, R. M., Morrison, A., Clevers, H. and Medema, R. H. (2005). FoxM1 is required for execution of the mitotic programme and chromosome stability. *Nat. Cell Biol.* **7**, 126-136.

LeBlanc, H. N., Tang, T. T., Wu, J. S. and Orr-Weaver, T. L. (1999). The mitotic centromeric protein MEI-S332 and its role in sister-chromatid cohesion. *Chromosoma* **108**, 401-411.

Liao, H., Winkfein, R. J., Mack, G., Rattner, J. B. and Yen, T. J. (1995). CENP-F is a protein of the nuclear matrix that assembles onto kinetochores at late G2 and is rapidly degraded after mitosis. *J. Cell Biol.* **130**, 507-518.

Liu, S. T., Hittle, J. C., Jablonski, S. A., Campbell, M. S., Yoda, K. and Yen, T. J. (2003). Human CENP-I specifies localization of CENP-F, MAD1 and MAD2 to kinetochores and is essential for mitosis. *Nat. Cell Biol.* **5**, 341-345.

Marston, A. L., Tham, W. H., Shah, H. and Amon, A. (2004). A genome-wide screen identifies genes required for centromeric cohesion. *Science* **303**, 1367-1370.

McCleland, M. L., Kallio, M. J., Barrett-Wilt, G. A., Kestner, C. A., Shabanowitz, J., Hunt, D. F., Gorbsky, G. J. and Stukenberg, P. T. (2004). The vertebrate Ndc80 complex contains Spc24 and Spc25 homologs, which are required to establish and maintain kinetochore-microtubule attachment. *Curr. Biol.* **14**, 131-137.

McGuinness, B. E., Hirota, T., Kudo, N. R., Peters, J. M. and Nasmyth, K. (2005). Shugoshin prevents dissociation of cohesin from centromeres during mitosis in vertebrate cells. *PLoS Biol.* **3**, e86.

Meraldi, P. and Sorger, P. K. (2005). A dual role for Bub1 in the spindle checkpoint and chromosome congression. *EMBO J.* **24**, 1621-1633.

Mitchison, T., Evans, L., Schulze, E. and Kirschner, M. (1986). Sites of microtubule assembly and disassembly in the mitotic spindle. *Cell* **45**, 515-527.

Moore, L. L., Morrison, M. and Roth, M. B. (1999). HCP-1, a protein involved in chromosome segregation, is localized to the centromere of mitotic chromosomes in Caenorhabditis elegans. *J. Cell Biol.* **147**, 471-480.

Morrow, C. J., Tighe, A., Johnson, V. L., Scott, M. I. F., Ditchfield, C. and Taylor, S. S. (2005). Bub1 and Aurora B cooperate to maintain BubR1-mediated inhibition of APC/CCdc20. *J. Cell Sci.* **118,** 3639-3652

Nasmyth, K. (2002). Segregating sister genomes: the molecular biology of chromosome separation. *Science* **297**, 559-565.

Ortiz, J., Stemmann, O., Rank, S. and Lechner, J. (1999). A putative protein complex consisting of Ctf19, Mcm21, and Okp1 represents a missing link in the budding yeast kinetochore. *Genes Dev.* **13**, 1140-1155.

Rabitsch, K. P., Gregan, J., Schleiffer, A., Javerzat, J. P., Eisenhaber, F. and Nasmyth, K. (2004). Two fission yeast homologs of Drosophila Mei-S332 are required for chromosome segregation during meiosis I and II. *Curr. Biol.* **14**, 287-301.

Rattner, J. B., Rao, A., Fritzler, M. J., Valencia, D. W. and Yen, T. J. (1993). CENP-F is a.ca 400 kDa kinetochore protein that exhibits a cell-cycle dependent localization. *Cell Motil. Cytoskeleton* **26**, 214-226.

Rieder, C. L. and Maiato, H. (2004). Stuck in division or passing through: what happens when cells cannot satisfy the spindle assembly checkpoint. *Dev. Cell* **7**, 637-651.

Salic, A., Waters, J. C. and Mitchison, T. J. (2004). Vertebrate shugoshin links sister centromere cohesion and kinetochore microtubule stability in mitosis. *Cell* **118**, 567-578.

Stear, J. H. and Roth, M. B. (2004). The Caenorhabditis elegans kinetochore reorganizes at prometaphase and in response to checkpoint stimuli. *Mol. Biol. Cell* **15**, 5187-5196.

Steensgaard, P., Garre, M., Muradore, I., Transidico, P., Nigg, E. A., Kitagawa, K., Earnshaw, W. C., Faretta, M. and Musacchio, A. (2004). Sgt1 is required for human kinetochore assembly. *EMBO Rep.* **5**, 626-631.

Tang, Z., Sun, Y., Harley, S. E., Zou, H. and Yu, H. (2004). Human Bub1 protects centromeric sister-chromatid cohesion through Shugoshin during mitosis. *Proc. Natl. Acad. Sci. USA* **101**, 18012-18017.

Tighe, A., Johnson, V. L., Albertella, M. and Taylor, S. S. (2001). Aneuploid colon cancer cells have a robust spindle checkpoint. *EMBO Rep.* **2**, 609-614.

Tighe, A., Johnson, V. L. and Taylor, S. S. (2004). Truncating APC mutations have dominant effects on proliferation, spindle checkpoint control, survival and chromosome stability. *J. Cell Sci.* **117**, 6339-6353.

Vogt, A., Sun, J., Qian, Y., Hamilton, A. D. and Sebti, S. M. (1997). The geranylgeranyltransferase-I inhibitor GGTI-298 arrests human tumor cells in G0/G1 and induces p21(WAF1/CIP1/SDI1) in a p53-independent manner. *J. Biol. Chem.* **272**, 27224-27229.

Wei, Y., Bader, D. and Litvin, J. (1996). Identification of a novel cardiac-specific transcript critical for cardiac myocyte differentiation. *Development* **122**, 2779-2789.

Yang, Z., Guo, J., Chen, Q., Ding, C., Du, J. and Zhu, X. (2005). Silencing mitosin induces misaligned chromosomes, premature chromosome decondensation before anaphase onset, and mitotic cell death. *Mol. Cell. Biol.* **25**, 4062-4074.

Zhu, X., Chang, K. H., He, D., Mancini, M. A., Brinkley, W. R. and Lee, W. H. (1995a). The C terminus of mitosin is essential for its nuclear localization, centromere/kinetochore targeting, and dimerization. *J. Biol. Chem.* **270**, 19545-19550.

Zhu, X., Mancini, M. A., Chang, K. H., Liu, C. Y., Chen, C. F., Shan, B., Jones, D., Yang-Feng, T. L. and Lee, W. H. (1995b). Characterization of a novel 350-kilodalton nuclear phosphoprotein that is specifically involved in mitotic-phase progression. *Mol. Cell. Biol.* **15**, 5017-5029.